

## **Effect of CaF<sub>2</sub> addition on the densification and the foaming of sintered glass-ceramics by metallurgical slag**

<sup>1</sup>Esmat M. A. Hamzawy, <sup>\*2</sup>Alexander Karamanov, <sup>1</sup>Hussein Darwish, <sup>2</sup>Emilia Karamanova

<sup>1</sup>Glass Research Department, National Research Centre, Dokki, P.C.12622, Cairo, Egypt

<sup>2</sup>Institute of Physical Chemistry, Bulgarian Academy of Sciences, Acad. G. Bonchev Str.,  
Block 11, 1113 Sofia, Bulgaria

### **Abstract**

In this study the possibility to use metallurgical slag from Egyptian company “Helwan” for the production of self-glazing sintered glass-ceramics or glass-ceramic foams is discussed. In details is highlighted the effect of CaF<sub>2</sub> addition (in amounts of 0, 2.5, 5 and 7.5 wt %) on the glass melting, densification and foaming processes.

The sintering and the bloating trends are evaluated by hot stage microscopy, HSM, using different heating rates and fraction sizes. The phase formation is estimated by X-ray diffraction, XRD, and scanning electron microscopy, SEM. The densities, the porosities and the structures of some of obtained samples are studied by gas pycnometry and mercury intrusion porosimetry.

The results demonstrate that the studied glass powders are characterized by good sinter ability in the interval 800-950°C and subsequent intensive bloating in the range 1050-1150°C.

The increasing of CaF<sub>2</sub> amount in the batches leads to a notable decrease of both melting and sintering temperatures. However, the maximal addition of 7.5 % leads to some reduction of the densification and foaming trends, which is consequence of more intensive liquid-liquid immiscibility and phase formation. Notwithstanding, self-glazed glass-ceramic with high percentage of CaF<sub>2</sub> and improved micro-hardness and crystallinity can be obtained by using finer glass powders, moderate heating rates and holding temperatures of 950-1000 °C.

At the same time, glass-ceramics foams with huge closed porosity of about 80 vol % can be synthesized using glass powders without or with modest addition of CaF<sub>2</sub> applying higher heating rates and holding temperatures of 1100-1150 °C.

**Keywords:** industrial wastes, glass-ceramics, sintering, foaming

\*corresponding author, e-mail: [karama@ipc.bas.bg](mailto:karama@ipc.bas.bg)

**Highlights:**

- Sintered glass-ceramic materials from metallurgical are studied.
- The effect of CaF<sub>2</sub> addition on melting, densification and foaming is elucidated.
- At high CaF<sub>2</sub> addition self-glazed material is obtained.
- At moderate CaF<sub>2</sub> addition glass-ceramic foams are obtained.

## 1. Introduction

The manufacture of different building glass-ceramics is a useful tool to resolve a part of the problems with the storage and the immobilization of various inorganic wastes [1-4]. The major part of these studies is related to residues arising from different metallurgical productions.

The first glass-ceramic by industrial wastes, named “Slagsitall”, is based on blast furnace slag. The industrial production of this material started in the Ex-Soviet Union after 1964-1966 and for three-four decades the total amount of produced “Slagsitall’s” tiles surpasses twenty billion square meters [4, 5]. Many similar products were subsequently developed in the UK, Poland, China and many other countries.

The slag is produced during the separation of molten iron from impurities in the steel-making furnaces. In the basic oxygen process hot liquid blast furnace metal, scrap and fluxes (as lime and dolomite) are charged to the converter at injection of high-pressure oxygen. The organic impurities from the charge form carbon oxides, while silicon, manganese, phosphorus and some iron react with the fluxes producing the steel slag. Thus, at the end of the refining operation, the liquid steel is tapped (poured) into a ladle whereas the slag is retained in the vessel and subsequently is tapped into a separate slag pot.

In the last decades the intensive studies with bulk glass-ceramics, sintered glass-ceramics and ceramics or glass-ceramic foams from different slag and other metallurgical residues has been successfully continued. Glass-ceramic was developed from Turkish blast furnace slag using 3 and 5 wt%  $\text{TiO}_2$  as nucleating agent [6]. Similar material was obtained mixing 57 wt% blast furnace slag with quartz sand, dolomite, limestone and clay [7]. In this case,  $\text{Cr}_2\text{O}_3$ ,  $\text{TiO}_2$ ,  $\text{CaF}_2$  and  $\text{LiF}$  were used to enhance the bulk crystallization. It was elucidated that  $\text{Cr}_2\text{O}_3$  and  $\text{TiO}_2$  act as better nucleation agent than  $\text{LiF}$  and  $\text{CaF}_2$  and that their addition leads to the formation of extremely fine-grained microstructure. Other glass-ceramics made from ferrous tailings and slag are applied as architectonic materials and in the chemical industry [8]. Bulk glass-ceramics can be also prepared from nickel slag, blast furnace slag and quartz sand [9]. Somewhat similar pyroxene material, based on 70 wt % electric arc furnace slag, was also synthesised by short one step crystallization treatment [10]. Glass-ceramic with a complex structure and main matrix, composed by pyroxene nano crystals, was obtained by huge amounts of problematic streams from Fe-Ni production [11]. Other materials with a fine-crystalline structure were also obtained from 90 wt % silicon manganese slag [12].

Glass–ceramic materials were successfully produced from steel slag using 31–41 wt% of the waste in the batch [13].

A low-cost technology was applied to prepare glass–ceramics through direct heat-treatment of molten glass, based on blast furnace slag and silica sand [14]. Other glass–ceramic from molten steel slag was also prepared using liquid–liquid mixing method: in this technique a mixture of additive powders in wt % (55 quartz powder, 5 Na<sub>2</sub>O, 16 emery powder, 15 CaO, 8 MgO, 1 TiO<sub>2</sub>) were melted at 1350°C separately and then mixed with a melt from steel slag [15].

On the other hand, ceramics, containing steel slag and glass cullet from energy saving lamps, were prepared by attrition milling in different proportions, pressing and fast firing at several temperatures in the range 1000–1140 °C. Some of the obtained samples appear suitable for the industrial production of floor tiles [16]. Using the conventional firing process, ceramic materials were produced from blast furnace slag alone or with combination of aluminum silicate minerals [17, 18]. Low-cost ceramics with good mechanical characteristics, with no traditional fluxes and 30, 50 and 70% blast furnace slag in the batches, were synthesized at sintering temperatures of 1200–1220 °C [19]. Materials with good properties were also successfully obtained by ceramic sintering of blast-furnace slag with addition of 5 wt% potash feldspar [20].

Many studies are also being carried out to obtain sintered or foamed materials by fine glass powders [4, 21]. Metallurgical slag, wastes of soda-lime silica glass and kaoline clay were used by sintering process up to 1050° C to form porous materials with porosity > 30 % [22]. Glass cullet and blast furnace slag as main batch raw materials and addition of SiC were used to form porous specimens with bulk density in the range 0.95 - 1.15 g/cm<sup>3</sup>. The authors found that the compressive strength of the resulting materials depend on the concentration of SiC and the used sintering temperature [23].

Using zeolitic rock from two different Russian deposits porous granulated materials were produced at temperatures below 900 °C. In this case, dolomite was used as carbonate expanding agents [24]. The obtained samples possesses a compressive strength of 8.8–15.7 MPa and a bulk density of 0.6–7 g/cm<sup>3</sup> .

In general, most of the glass foams are fabricated by sintering of glass powders mixed with foaming agents (carbon black, graphite, SiC and different organic substances or various carbonites as CaCO<sub>3</sub>, Na<sub>2</sub>CO<sub>3</sub> or dolomite) releasing gasses in the pyroplastic mass formed during the softening of sintering matrix [25-27].

An alternative mechanism of self-foaming is observed in many iron-rich glass powders. In this case, the formation of glass-ceramic foam is connected to the oxygen release due to reduction of  $\text{Fe}^{+3}$  into  $\text{Fe}^{+2}$  at higher temperature [21, 28]. Other interesting example for foaming due to realize of  $\text{O}_2$  is the reduction of  $\text{MnO}_2$  to  $\text{Mn}_2\text{O}_3$  [29, 30].

However, when the bloating trend is reduced, sintered self-glazed ceramics or glass-ceramics might be also developed using fine glass powders. For example, self-glazed samples were obtained by glass rejects and iron and steel wastes [4, 22]. Self-glazed ceramic material was also prepared from recycled glass, residues from ceramic industry and silica sand [31]; the products were characterized with a high hardness, density and good chemical durability.

In the present work, rich of BaO metallurgical slag, which contain simultaneously high amount of iron and manganese oxides, is used to obtain sintered glass-ceramics and/or glass-ceramics foams. The effect of  $\text{CaF}_2$  additions (2.5, 5 and 7.5 wt %) on the melting, the densification and the foaming is also elucidated.

## 2. Experimental Procedures

In this study a slag from iron and steel company “Helwan”, which is located on the border of Cairo governorate, was used to synthesize sintered glass-ceramics and glass-ceramic foams. The slag production of this plant is at about 30000 tons/year; it is collected in piles, which are spread around the factory. Since this slag contains relatively low amount of glass-formers ( $\text{SiO}_2 + \text{Al}_2\text{O}_3$ ) the main glass batch was obtained by mixing 70 wt % slag with 30 wt % industrial sand. In addition, in thus obtained batch were added 2.5, 5 or 7.5 parts  $\text{CaF}_2$ , respectively. The resulting glass compositions (labelled **H-0**, **H-2.5**, **H-5** and **H-7.5**, respectively) together with such from used slag and sand are summarized in Table 1.

The chemical composition of the slag is typical for these wastes, excluding the relatively high amounts of BaO and MnO [1-4]. These oxides however can be considered as a potential fluxes, which can favour the melting procedure.

The x-ray diffraction pattern of the slag highlight quartz, gehlenite [ $\text{Ca}_2\text{Al}(\text{AlSi}_2)\text{O}_7$  - JCPDS Nr79-242], barium iron oxide [ $\text{BaFeO}_{2.6}$  - JCPDS Nr39-183] and traces of kirschsteinite [ $\text{CaFeSiO}_4$ - JCPDS Nr 34-98]. In the XRD pattern an amorphous halo is also well distinguished, which elucidate the presence of high amount of glassy phase.

The parent batches in amounts of about 150g were melted using corundum crucibles and electric furnace. Dark brown glasses were obtained after 2 h melting within 1350 to 1450 °C temperature range. The melting temperature decreases gradually with the increasing of

CaF<sub>2</sub> addition in the batch (i.e. the composition **H-0** was melted at 1450 °C, while **H-7.5-** at 1350 °C). Thus obtained melts were water quenched and the resulting frits were crashed and milled below 125 µm.

The thermal behaviour of glasses was evaluated by DTA technique (Perkin Elmer – Diamond) using about 10 mg bulk and powder samples at heating rate of 20°C/min.

The sinter-ability and the foaming trends were studied by hot stage microscopy (HSM) at non-isothermal experiments at 20°C/min using HSM 1400 - Misura (ESS - Italy). Additionally, in order to estimate the optimal holding times, some isothermal runs were also done. Since the HSM technique gives fast and realistic results in the last decade it was effectively used for similar studies by different research groups [32, 33].

Various thermal treatments were carried out also in electric furnace using pressed at 20 kN cylindrical samples with initial diameter of 25 mm.

The phases identification of used slag, parent glasses and different samples, obtained at various heat-treatments, were made by X-ray powder diffraction (XRD, D8-Advance, Bruker, Germany) using Cu K-radiation.

The crystalline structure of samples was examined on fresh fractured surfaces after 5 seconds etching with 2 % HF by scanning electron microscopy (SEM - JEOL JSM 6390, Japan).

The absolute densities of parent glasses, after crashing below 5 mm, and apparent densities of obtained sintered glass-ceramic samples were measured using gas pycnometer (AccyPy1330, Micromeritics, USA) in argon atmosphere. The closed porosity,  $P_c$ , was estimated through the relation:

$$P_c \text{ (vol\%)} = 100 * (\rho_c - \rho_s) / \rho_c$$

where  $\rho_c$  is the density of crashed glass and  $\rho_s$  is the density of sintered sample.

The micro-hardness of these samples was determined using Vicker's Microhardness Tester (HMV, Shimadzu, type M, Japan).

Finally, the total porosity and the apparent density of some of the obtained foams was evaluated by mercury intrusion porosimetry pore size analyser (Model: 99320 v2.08 Micromeritics, USA). In this method the specimen was placed in a pentameter and infused with mercury under increasing pressure.

### **3. Results and Discussions**

#### **3.1 Evaluation of sintering and foaming trends**

The XRD analyses of obtained frits confirm their amorphous structures. The DTA tests with bulk samples show no evident exo-crystallization and endo-melting effects which elucidate that the glasses are characterized by a scarce tendency for bulk crystallization. For this reason only the possibility to obtain sintered glass-ceramics or glass-ceramics foams were investigated.

The sinter-ability and the subsequent foaming trend of the four glass powders ( $< 125 \mu\text{m}$ ) were tested by HSM experiments and the results are shown in Figures 1 and 2, respectively. The data for the sintering tendency in the low temperature interval (600-900 °C) were obtained at a regime of high magnification of the apparatus camera, while in the range 900-1250 °C, due to intensive increase of the sample volume, a regime at lower magnification was used. In Figure 3 are shown some images of sample **H-5**: the photos corresponding to 25 °C (**a**), to the beginning of sintering at  $\sim 770^\circ\text{C}$  (**b**) and to its end at  $\sim 900^\circ\text{C}$  (**c**) are captured at high magnification, while these corresponding to the beginning of foaming at  $\sim 1070^\circ\text{C}$  (**d**), to its maximal expansion at  $\sim 1140 \text{ }^\circ\text{C}$  (**e**), as well as to the characteristic temperature “melting points” at  $\sim 1200 \text{ }^\circ\text{C}$  - at low magnification.

Figure 1 demonstrates that the sintering starts in the interval 750-800 °C and completes in the range 850 – 930 °C. It is evident that, due to the viscosity drop, the increasing of  $\text{CaF}_2$  amount decreases the sintering temperatures. At the same time, the maximal degree of densification decreases with the rise of  $\text{CaF}_2$  amount. In sample **H-0** the shrinkage at 930 °C is  $\sim 27 \%$  which corresponds to a very good degree of sintering, while in sample **H-7.5** the maximal reached shrinkage at 850 °C is only  $\sim 12\%$ . This low value indicates that the densification is not completed and that open porosity remains in this sample.

The decreasing of densification trend with the increasing of  $\text{CaF}_2$  percentage probably might be explained by a rise of the tendency for liquid-liquid separation. It is well known that the addition of  $\text{CaF}_2$  in silicate glasses leads to an immiscibility below the melting temperatures [34]; often this liquid-liquid separation provokes subsequent crystallization. The both processes increase the apparent viscosity, which can influence negatively on the sintering ability.

Figure 2 shows an intensive foaming in the temperature interval 1070-1170 °C. In this case the addition of  $\text{CaF}_2$  decreases the maximal foaming temperature but the effect is not comparable to the diminishing of the sintering temperature. In addition, sample **H-7.5** demonstrates a significantly lower “foaming” ability, which can be explained by its lower degree of sintering and the presence of open pores.

After the foaming the samples start to “collapse”, which means that after 1150-1170 °C the formed crystal phases rapidly melt. Higher is the CaF<sub>2</sub> amount faster is this drop. As a result, the “melting points” of samples **H-0**, **H-2.5**, **H-5** and **H-7.5** occur at about 1225, 1215, 1200 and 1180 °C, respectively. The temperature variation of 40-50 °C between the “melting points” of compositions **H-0** and **H-7.5** is similar to the one, observed in the sintering intervals, which again demonstrates the strong effect of CaF<sub>2</sub> addition on the viscosity diminishing.

In order to elucidate better the sintering and the foaming trends, additional experiments with bigger 25 mm cylindrical samples were made in an electrical furnace. These specimens were heat-treated at 10°C/min and held for 3 minutes at 1000, 1025 and 1050 °C; their images are presented in Figure 4. These additional tests confirm and complete the HSM experiments. The composition **H-7.5** appear more “crystalline”, it show an open porosity at 1000 and 1025 °C, while at 1050 °C its bloating is not so intensive as in the other three compositions. At the same time **H-0** show a bright smooth surface without open pores yet at 1000 °C, its deformation at 1025 °C is rigorous and at 1050 °C it shows the best foaming trend. Compositions **H-2.5** and **H-5** have similar behaviour, but their deformation starts earlier: **H-5** sample becomes spherical already at 1000 °C.

### 3.2 Sintered glass-ceramics obtained at lower temperature

The foaming tendency depends on the kind of formed porosity before the beginning of bloating. If the gassy phase is formed in a structure with predominantly open porosity its effect on the foaming is not so remarkable.

It is well known that the sinter-ability of glass-ceramics powders (i.e. the trend to form samples without open porosity) is improved by using finer glass fractions and/or higher heating rate [4, 25]. For these reasons, additional HSM experiments with composition **H-0** and **H-7.5** were performed. The glass powders were milled additionally below 54 µm and runs at 5 °C/min and 30 °C/min were done.

The obtained results are shown in Figure 5. The decreasing of particles size significantly improves the densification (especially for composition **H-7.5**), while the foaming effect becomes more intensive at the higher heating rate.

This effect is particular in composition **H-7.5**, where at the low heating rate practically no bloating is observed. In addition, the temperatures of sintering intervals at 5 and 30 °C/min practically overlap which is a very unusual behaviour. These peculiarities might be explained, assuming that at a reduced heating rate the expected liquid-liquid separation and/or phase



formation are taking place at lower temperatures, which leads to an earlier increase of the apparent viscosity.

In composition **H-0**, where an intensive immiscibility is not expected, the densification processes are “regular” (i.e. lower is the heating rate, lower is the sintering temperature). It can be also noted, that due to better sintering the foaming starts at lower temperature at the higher heating rate.

After that, additional experiments with 25 mm cylindrical samples of the four glass powders were made in electric furnace using different heating rates and holding temperatures. This research confirms the trends, shown in Figure 5, and highlight that with variations of the fraction size, the heating rate and the holding temperatures different products might be manufactured.

For an example, by using fine glass powders, moderate heating rates and holding temperatures below the foaming interval, well sintered samples with a self-glazed surface and zero water soaking can be manufactured. In Table 2 are shown images of specimens, obtained using fractions below 38  $\mu\text{m}$ , heating rate of 10  $^{\circ}\text{C}/\text{min}$  and 3 min holding at 1000  $^{\circ}\text{C}$ . In the Table are also reported the apparent densities of these samples, the absolute densities of the corresponding parent glasses, the resulting closed porosities and the hardness of obtained sintered glass-ceramics. The XRD patterns of these specimens are presented in Figure 6.

It is evident that the tendency for bloating decreases with the increasing of  $\text{CaF}_2$  amount, which logically leads to a higher density and a lower porosity. Sample **H-7.5** is characterized by an apparent density of 2.57  $\text{g}/\text{cm}^3$  and ~5 % closed porosity, while in **H-0** the apparent density is only 2.22  $\text{g}/\text{cm}^3$  and the closed porosity reaches ~16 %.

The relatively high closed porosity in **H-0** was confirmed by SEM. Figure 7-a shows a fracture, which highlights very well sintering body together with an elevated amount of spherical pores with different sizes. Figure 7-b elucidates the formation of crystal with 2-5 micron size, embedded in the main amorphous matrix. Here, it can be noted that the porosity in all samples, reported in Table 2, can be increased by 2-3 % due to rise of the absolute density during the crystallization [35]. In fact, at moderate crystallization of 20-30 % pyroxenes the absolute density increases with at about 0.1-0.15  $\text{g}/\text{cm}^3$ .

Figure 7 presents the XRD results, which show intensive amorphous halos and formation of pyroxene phase, similar to hendenbergite ( $\text{CaFeSi}_2\text{O}_6$ , JCPDS Nr-2425). The addition of  $\text{CaF}_2$  leads to some increasing in the crystallinity and of traces of cristobalite in **H-7.5**. The photos from Table 2 elucidate that this increasing of crystallinity effects on the glossy appearance of the samples.

The rise in crystallinity, coupled with the lower porosity, increases the micro hardness from 490 kg/mm<sup>2</sup> of **H-0** to 521 kg/mm<sup>2</sup> of **H-7.5**. These values are significantly higher than those of the natural marbles and are similar to the high quality granites.

### **3.3 Sintered glass-ceramic foams, obtained at high temperature**

Since the composition **H-7.5** is characterized by a reduced bloating trend it was not investigated for synthesis of glass-ceramic foams. In addition, in order to demonstrate better the effect of CaF<sub>2</sub> addition, the studied three foams were obtained at heat-treatment, corresponding to the optimal regime for composition **H-5**.

The optimal holding temperatures and times to obtain stable **H-5** glass-ceramic foams with fraction below 125 microns, were estimated at heating rates of 20 °C/min and 20 minutes isothermal HSM runs at different temperatures. These results highlight that the optimal temperatures are in the interval 1100-1120 °C, where the foaming completes for 5-20 minutes. At lower temperatures the bloating effect was not so intensive, while at higher - rapid collapse of the samples were observed after only 1-2 minutes.

In Figure 8-a isothermal HSM plot at 1120 °C is shown, while in Figure 8-b representative images after overall heat-treatments of 40, 50, 60 and 70 min are presented. The sintering starts at about 800 °C (after ~ 40 min heat-treatment) and completes for 5 min at about 900 °C; the foaming starts at about 1050°C. In the beginning of the isothermal step (i.e. after ~ 55 min overall heat-treatment) the expansion value is already ~115 % and for 5 min holding it reaches ~140 %. Then the expansion decreases a little, but the sample remains stable. No changes are observed also during the cooling, which indicates that the formed glass-ceramic foam might be considered as a fire resistant material up to 1050-1100 °C. This elucidates that at 1100-1120 °C crystal phases yet are presented in the sample; otherwise, fast collapse can be observed.

This assumption was established with DTA runs of the three glass powders, which results are presented in Figure 9. The plots show glass transition temperatures in the range 690-740 °C (which is a good agreement with the sintering curves in Figure 1) and loose exo-effects with low intensity in the range 800-950 °C (probably due to oxidation [35] and low intensity surface crystallization). However, the endo-effects are more intensive, their onset temperatures (i.e. the eutectic temperatures) are at 1090-1120 °C, while the endo-peak temperatures at 1130-1160 °C practically coincide with the foaming temperatures from Figure 2. This overlapping confirms that the intensive bloating process is related to a partial melting of the formed during the heating crystal phases. The high temperature interval of foaming also

indicates that the mechanism of gas formation is related to oxygen release due to Fe<sup>3+</sup> and/or Mn<sup>3+</sup> reduction [28-30].

After these HSM and DTA tests, 25 mm cylindrical samples of the three glass powders were heat-treated in electric furnace at 20 °C/min and hold for 10 minutes at 1110 °C. The apparent densities and the porosities of thus obtained specimens were estimated by mercury intrusion porosimetry and the results are reported in Table 3. It is evident that, at used short heat-treatment, the addition of CaF<sub>2</sub> leads to an increase of the porosity, which might be explained mainly by the decreasing of viscosity of the residual melt. The reached value of ~80 % porosity, coupled with the good crystallinity of the sample, can be considered as very satisfactory result [4, 21].

The XRD patterns of these glass-ceramic foams are shown in Figure 10 and highlight that the crystallinity is higher than that in the self-glassed samples, obtained at 1000 °C. This difference is more evident for compositions **H-0** and **H-5**. For **H-0**, in accordance with the corresponding DTA result, it might be assumed that the partial pyroxene melting at 1110 °C is negligible, while in **H-5**, due to the higher percentage of CaF<sub>2</sub>, probably more intensive crystallization process is taking place during the cooling.

These porosity and XRD results were confirmed by SEM observations. In Figure 11 are presented some typical images of the studied samples. The comparison between samples **H-0** (*a*) and **H-5** (*c*) highlighted the significant increase of the porosity in **H-5**, while the confront between samples **H-2.5** (*b*) and **H-5** (*d*) at higher magnification shows the differences in their crystallinities.

## Conclusions

The possibilities to obtain self-glazed sintered glass-ceramics and/or glass-ceramic foams by metallurgical slag and industrial sand is highlighted. In order to decrease the cost of these products, the effect of 2.5, 5 and 7.5 wt %  $\text{CaF}_2$  addition in the batch on glass melting, densification, crystallization and bloating is also established.

The increase of  $\text{CaF}_2$  amount leads to a notable decrease of both melting and sintering temperatures. In addition, the variations of  $\text{CaF}_2$  percentage, fraction size, heating rate and holding temperatures lead to differences of sintering trend, phase formation and foaming ability.

In general, the studied glass powders (below 125  $\mu\text{m}$ ), are characterized by a good sinter ability in the interval 800-950°C and intensive foaming in the range 1050-1150°C. However, in the composition with 7.5 %  $\text{CaF}_2$  reductions of the densification and bloating trends are observed. Notwithstanding, when finer glass powder of this composition is used and moderate heating rates are applied self-glazed sintered glass-ceramic with improved micro-hardness and crystallinity can be obtained at holding temperatures of 980-1000 °C.

At the same time, glass-ceramic foams with huge porosity of about 80 vol % can be synthesized by using the compositions with modest  $\text{CaF}_2$  addition. In this case, higher heating rates and holding temperatures of 1100-1130 °C can be applied.

**Acknowledgements:** The work is supported by Project H19/7 “Theory and application of sinter-crystallization” (National Science Fund of Bulgaria) and by Project “Iron-rich glass-ceramics foams, glass-ceramics and ceramics from industrial wastes” (Joint Research project between National Research Centre of Egypt and Bulgarian Academy of Sciences).

## References

1. Donald, I.W.: Waste immobilization in glass and ceramic based hosts: radioactive, toxic, and hazardous wastes. John Wiley & Sons (2010)
2. Rawlings, R.D., Wu, J.P., Boccaccini, A.R.: Glass-ceramics: Their production from wastes - a Review. *J. Mater. Sci.* 41, 733-761 (2006)
3. Colombo, P., Brusatin, G., Bernardo, E., Scarinci, G.: Inertization and reuse of waste materials by vitrification and fabrication of glass-based products. *Curr. Opin. Solid St. Mat.* 7, 225-239 (2003)
4. Rincón, A., Marangoni, M., Cetin, S., Bernardo, E.: Recycling of inorganic waste in monolithic and cellular glass-based materials for structural and functional applications., *Chem. Technol. Biotechnol.* 91,1946–1961 (2016)
5. Pavlushkin, N.M.: Chemical technology of glass and glass-ceramics (in Russian). Strojizdat, Moscow (1983)
6. Ovecoglu, M.L.: Microstructural Characterization and Physical Properties of a Slag – Based Glass Ceramic Crystallized at 950 and 1000°C. *J. Euro. Ceram. Soc.* 18, 161-168 (1998)
7. Khater, G.A.: Influence of Cr<sub>2</sub>O<sub>3</sub>, LiF, CaF<sub>2</sub> and TiO<sub>2</sub> nucleants on the crystallization behavior and microstructure of glass-ceramics based on blast-furnace slag. *Ceram. Int.* 37, 193-2199 (2011)
8. Liu, C., Shnip, Y., Zhang, D. Y., Jiang, M.: Development of Glass Ceramics Made From Ferrous Tailings and Slag in China. *J. Iron and Steel Res.* 14, 73-78 (2007)
9. Wang, Z.J., Ni, W., Li, K.Q., Huang, X.Y., Zhu, L.P.: Crystallization characteristics of iron-rich glass ceramics prepared from nickel slag and blast furnace slag. *Int. J. of Minerals, Metallurgy and Materials*, 18, 455-459 (2011)
10. Kamusheva, A., Hamzawy, E.M., Karamanov, A.: Crystallization and structure of glass-ceramic from electric arc furnace slag. *J. Chem. Technology and Metallurgy.* 50, 512-519 (2015)
11. Karamanov, A., Paunović, P., Rangelov, B., Ljatif, E., Kamusheva, A., Načevski, G., Karamanova, E. and Grozdanov, A.: Vitrification of hazardous Fe-Ni wastes into glass-ceramic with fine crystalline structure and elevated exploitation characteristics. *J. Env. Chem. Engineering.* 1, 432-441 (2017)
12. Khater, G.A.: The Use of Saudi Slag for the Production of Glass – Ceramic Materials, *Ceram. Inter.* 28, 59-67 (2002)
13. Feng, H., Yu, F., Junlin, X., Jun X.: Fabrication and characterization of glass–ceramics materials developed from steel slag waste, *Materials & Design.* 42, 198-203 (2012)
14. Yan, Z.D., Chen, Y., Bi, Y., Bi M. L., Mujun L.: Preparation of low cost glass–ceramics from molten blast furnace slag. *Ceram. Int.* 38, 2495-2500 (2012)
15. Zhang, K., Liu, J., Liu, W., Yang, J.: Preparation of glass-ceramics from molten steel slag using liquid-liquid mixing method. *Chemosphere* 85, 689-92 (2011)
16. Furlani, E., Tonello, G., Maschio, S.: Recycling of steel slag and glass cullet from energy saving lamps by fast firing production of ceramics. *Waste Manag.* 30, 1714-1719 (2010)

17. Mostafa, N., Shaltout, A., Shaltout, M., Abdel-Aal, M., El-Maghraby A.: Sintering mechanism of blast furnace slag–kaolin ceramics. *Materials and Design* 31, 3677-3682 (2010)
18. Ghosh, S., Das, M., Chakrabarti, S., Ghatak, S.: Development of ceramic tiles from common clay and blast furnace slag. *Ceram. Int.* 28, 393-400 (2002)
19. Karamanova, E., Avdeev, G. and Karamanov, A.: Ceramics from blast furnace slag, kaolin and quartz. *J. Europ. Ceram. Soc.* 31, 989-998 (2011)
20. Liu, H., Lu, H., Chen D., Wang. H., Xu, H., Zhang R.: Preparation and properties of glass–ceramics derived from blast-furnace slag by a ceramic-sintering process. *Ceram. Int.* 35, 3181-3184 (2009 )
21. Chinnam, R. K., Francis, A.A., Will, J., Bernardo, E., Boccaccin,i A.R. Review. Functional glasses and glass-ceramics derived from iron rich waste and combination of industrial residues. *J. Non-Cryst. Solids* 36, 563-574 (2013)
22. Ponsot, I., Bernardo, E. Self-glazed glass ceramic foams from metallurgical slag and recycled glass. *J. Cleaner Production* 59, 245–250 (2013)
23. Francis, A.A., Abdel Rahman, M.K., Daoud, A.: Processing, structures and compressive properties of porous glass-ceramic composites prepared from secondary by-product materials. *Ceram. Int.* 39, 7089–7095 (2013)
24. Volland, S., Vereshchagin, V.: Cellular glass ceramic materials on the basis of zeolitic rock, *Construction and Building Materials* 36, 940–946 (2012)
25. Scarinci, G., Brusatin, G., Bernardo, E.: Glass foams, in: M. Scheffler, P. Colombo (Eds.), *Cellular Ceramics: Structure, Manufacturing, Properties and Applications*, Wiley–VCH, Weinheim, pp. 158–176 (2005)
26. Chen, B., Wang, K., Chen X., Lu, A.: Study of Foam Glass with High Content of Fly Ash Using Calcium Carbonate as Foaming Agent. *Mater. Lett.* 79, 263-267 (2012)
27. Yi-Chong, L., Chi-Yen, H.: Glass foam from the mixture of reservoir sediment and  $\text{Na}_2\text{CO}_3$ . *Ceram. Int.* 38, 4415-4419 (2012)
28. Appendino, P., Ferraris, M., Matekovits, I., Salvo, M.: Production of glass ceramic bodies from the bottom ashes of municipal solid waste incinerators. *J. Eur. Ceram. Soc.* 24, 803-810 (2004)
29. Rasmus, R. König, P.J.. Yue, Y.: The mechanism of foaming and thermal conductivity of glasses foamed with  $\text{MnO}_2$  . *J. Non Cryst Solids* 425, 74 - 82 (2015)
30. García-Ten, J., Saburit, A., Orts, M.J., Bernardo, E., Colombo, P.: Glass foams from oxidation/reduction reactions using SiC,  $\text{Si}_3\text{N}_4$  and AlN powders: *Glass Technology: Europ. J. Glass Sci. Techn. Part A.* 52, 103-110 (2011)
31. Binhussain, M.A., Hamzawy, E.M., Alharbi, O.A.: Self glazed ceramic/glass composite and method for manufacturing the same. US patent, Application 20140179506 A1, 6/26/2014 (2014)
32. Sasmal, N. Garai, M., Karmakar, B.: Preparation and characterization of novel foamed porous glass-ceramics, *Mat. Characterization.* 103, 90–100 (2015)
33. Fiocco L., Elsayed H., Daguano J.K., Soares V.O, Bernardo E.; Silicone resins mixed with active oxide fillers and Ca–Mg Silicate glass as alternative/integrative precursors for wollastonite–diopside glass-ceramic foams, *J. Non-Cryst. Solids* 416, 44–49 (2015)
34. Vogel, W.; *Glass Chemistry*, Second Edition, Springer-Verlag, Berlin (1994)





35. Karamanov, A., Pelino, M.: Crystallization phenomena in iron-rich glasses, *J. Non-Cryst. Solids* 281 139-152 (2001)

**Table 1 . Chemical compositions of used raw materials and resulting glasses**

Sample No	SiO <sub>2</sub>	Al <sub>2</sub> O <sub>3</sub>	Fe <sub>2</sub> O <sub>3</sub>	CaO	MgO	MnO	BaO	TiO <sub>2</sub>	Cr <sub>2</sub> O	K <sub>2</sub> O	Na <sub>2</sub> O	SO <sub>3</sub>	P <sub>2</sub> O <sub>5</sub>	CaF <sub>2</sub>
HHS	28.7	7.0	7.6	25.9	1.5	8.1	15.2	1.0	0.06	0.9	0.5	2.7	0.07	
S	99.4	0.3	0.1											
H-0	49.2	5.1	5.5	18.6	1.1	5.8	10.9	0.7	0.04	0.7	0.4	1.9	0.05	--
H-2.5	46.7	4.9	5.2	17.7	1.1	5.5	10.3	0.7	0.04	0.6	0.4	1.8	0.05	1.7
H-5.0	45.9	4.8	5.1	17.4	1.0	5.4	10.2	0.7	0.04	0.6	0.4	1.8	0.05	3.4
H-7.5	45.7	4.7	5.0	17.3	1.0	5.3	10.1	0.0	0.04	0.6	0.4	1.8	0.05	7.0



**Table 2. Properties of self-glazed glass-ceramics**

	Absolute density	Apparent density	Porosity	Hardness	
	g/cm <sup>3</sup>	g/cm <sup>3</sup>	vol %	kg/mm <sup>2</sup>	
<b>H-0</b>	2.63±0.05	2.22±0.05	15±1	490	
<b>H-2.5</b>	2.67±0.05	2.47±0.05	8±1	503	
<b>H-5.0</b>	2.68±0.05	2.54±0.05	6±1	510	
<b>H-7.5</b>	2.70±0.05	2.57±0.05	5±1	521	

**Table 3. Apparent density and porosity of the glass-ceramic samples, obtained by mercury intrusion porosimetry.**

Sample	Density (g/cm <sup>3</sup> )	Porosity (vol. %)
<b>H-0</b>	1.29	52.2
<b>H-2.5</b>	0.89	64.3
<b>H-5.0</b>	0.54	82.0

## Figure captions

Figure 1. HSM plots in the sintering interval.

Figure 2. HSM plots in the foaming interval.

Figure 3. HSM images of composition **H-5** at 25 °C (a), 770 °C (b), 900 °C (c), 1070 °C (d), 1140 °C (e) and 1200 °C (f).

Figure 4. Images of samples sintered in electric furnace for 3 minutes holding time.

Figure 5. Sintering HSM plots of fine glass powder of compositions **H-0** and **H-7.5** at 5 and 30 °C/min

Figure 6. X-ray diffraction patterns of the sintered glass-ceramics at 1000 °C.

Figure 7. SEM images of fracture of sample **H-0**, sintered at 1000 °C.

Figure 8. Isothermal HSM plot of composition **H-5** at 1120 °C (a) and representative images after overall heat-treatments of 40, 50, 60 and 70 min.

Figure 9. DTA curves of **H-0**, **H-2.5** and **H-5** glass powders.

Figure 10. X-ray diffraction patterns of the glass-ceramic foams at 1110 °C.

Figure 11. SEM images of fracture of glass-ceramic foams **H-0** (a), **H-2.5** (b) and H-5 (c and d).

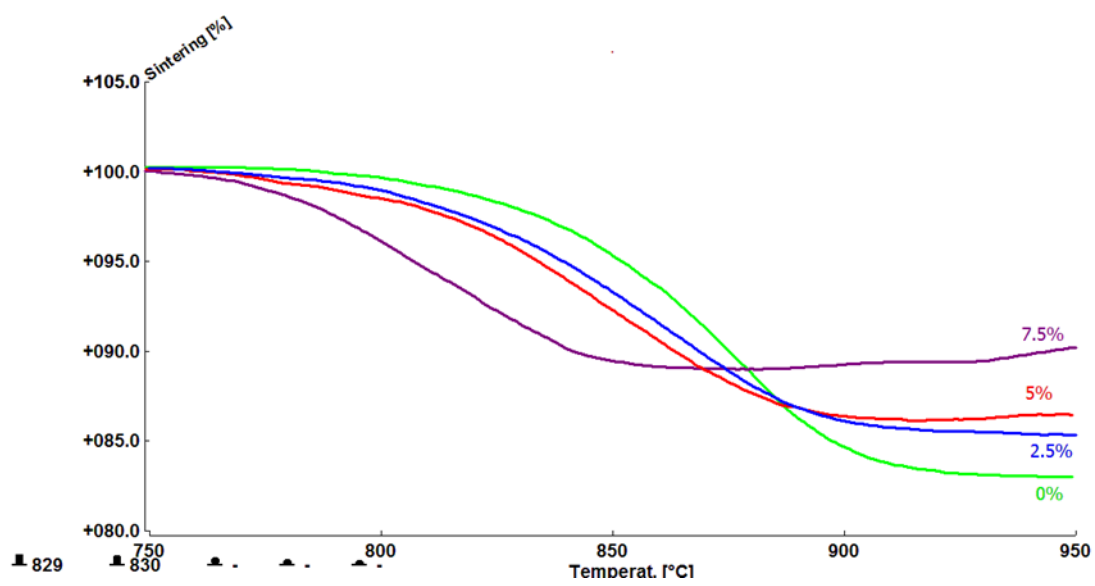


Fig. 1

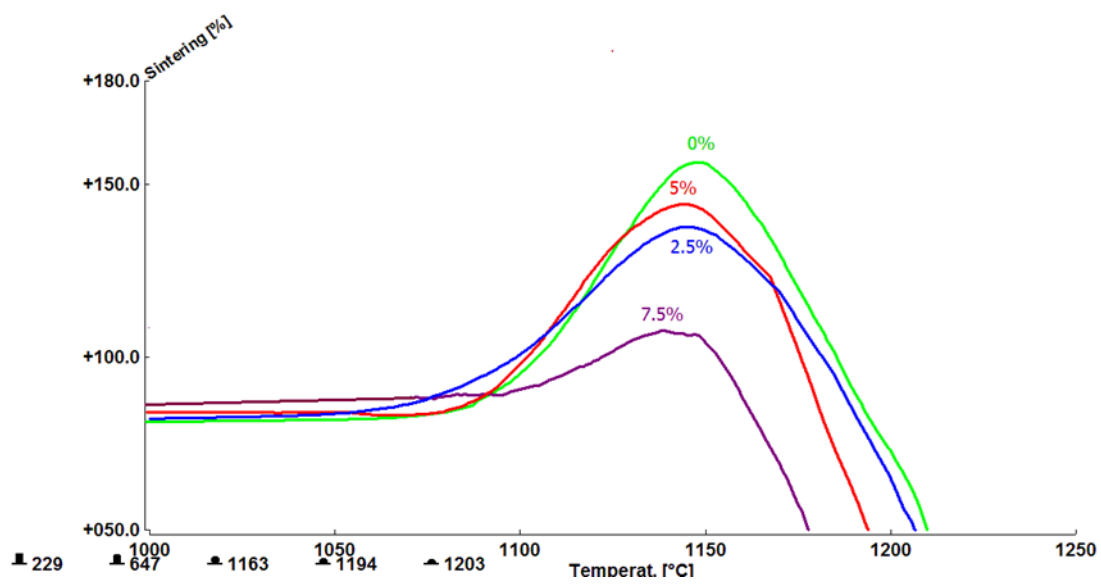


Fig. 2

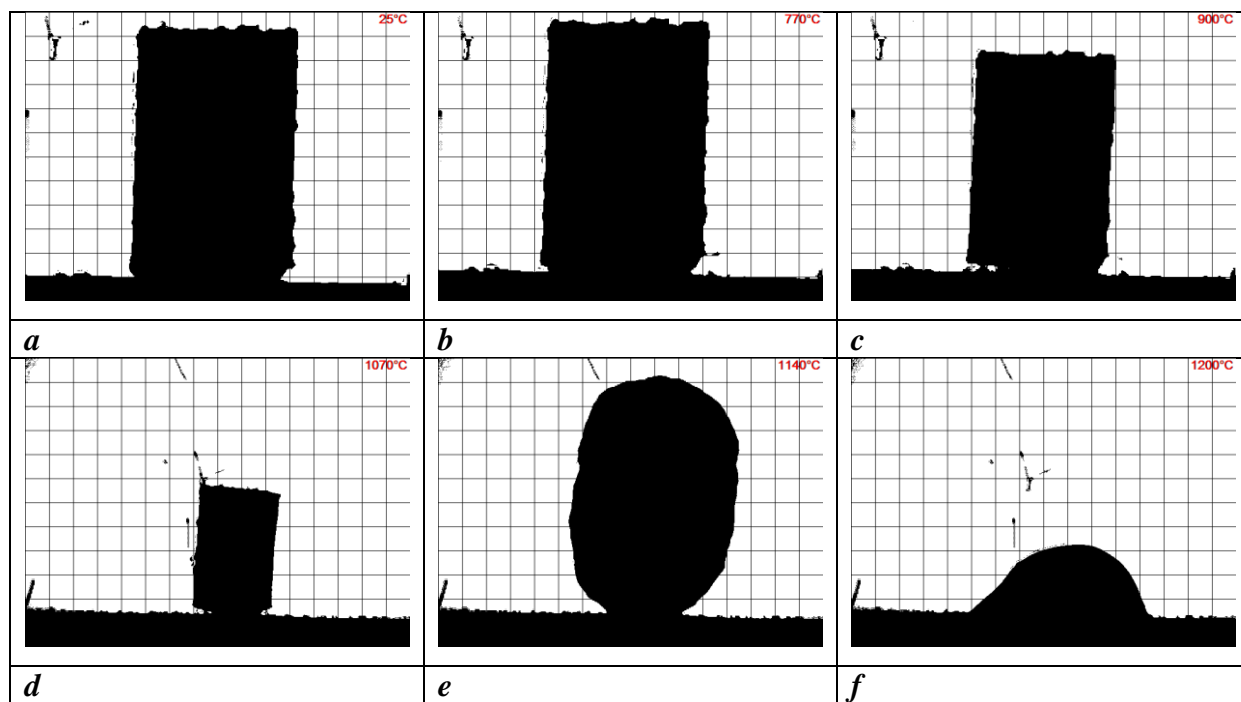


Fig. 3

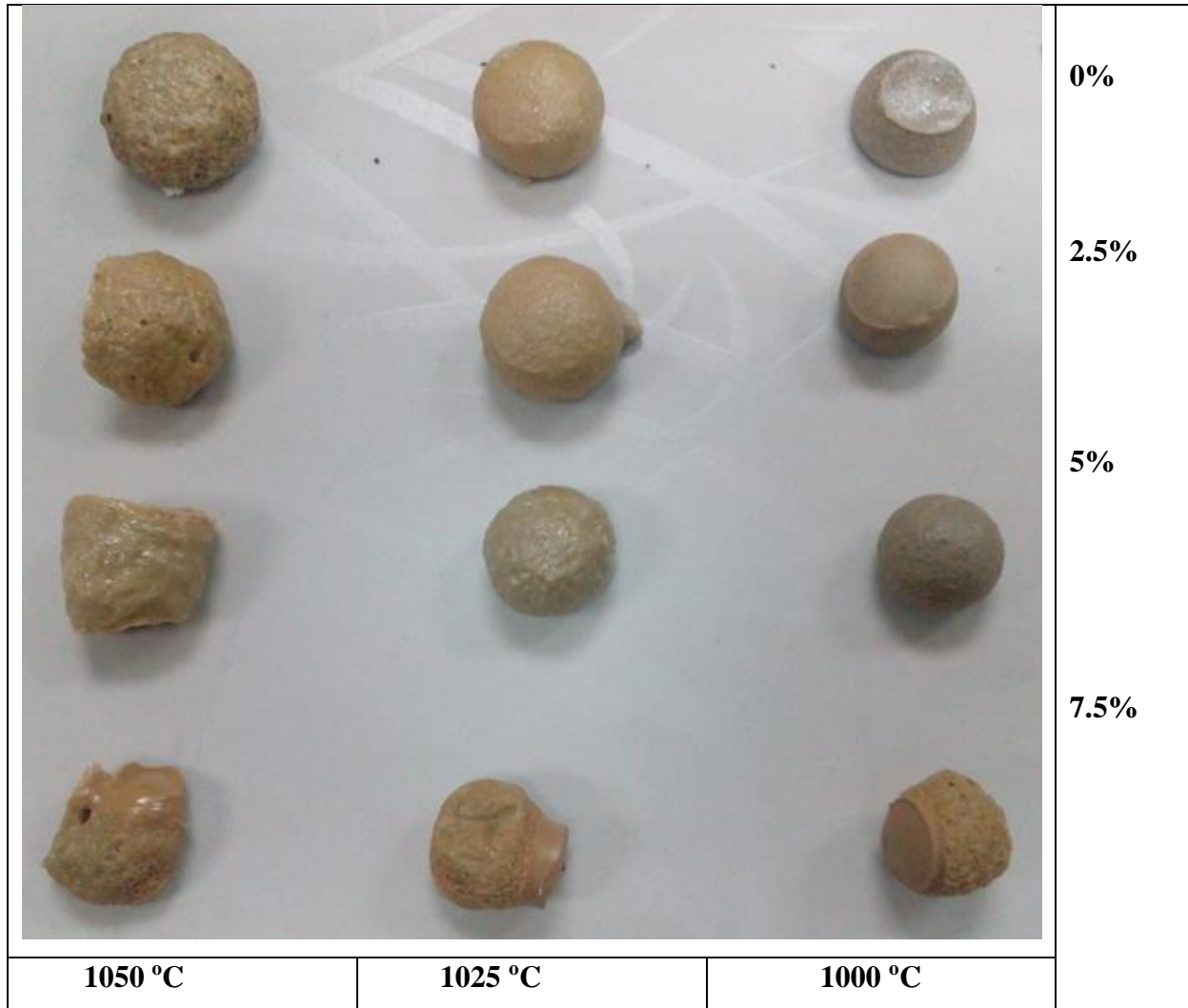


Fig. 4

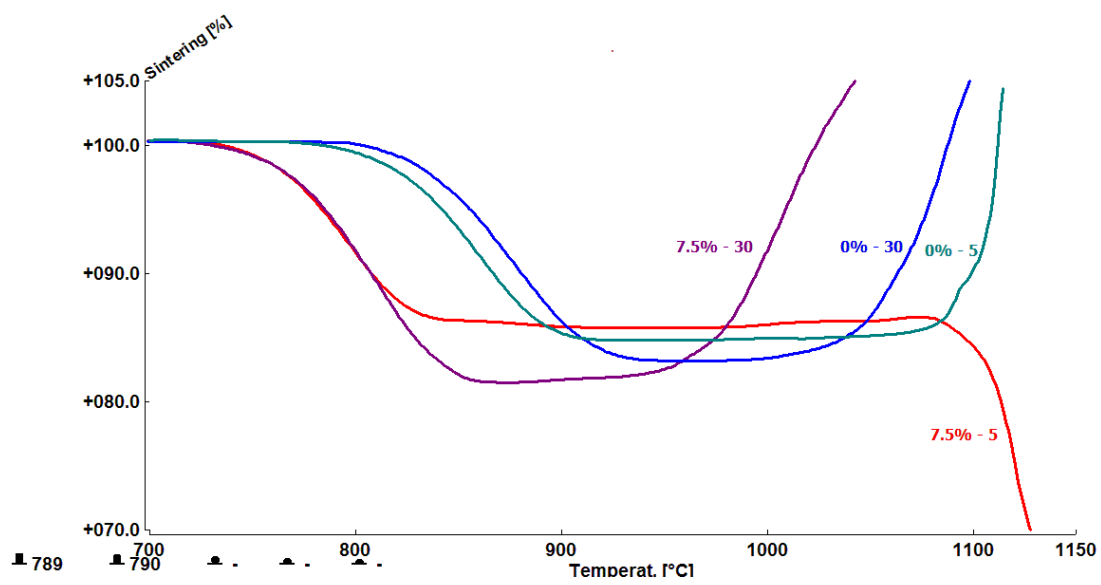


Fig. 5



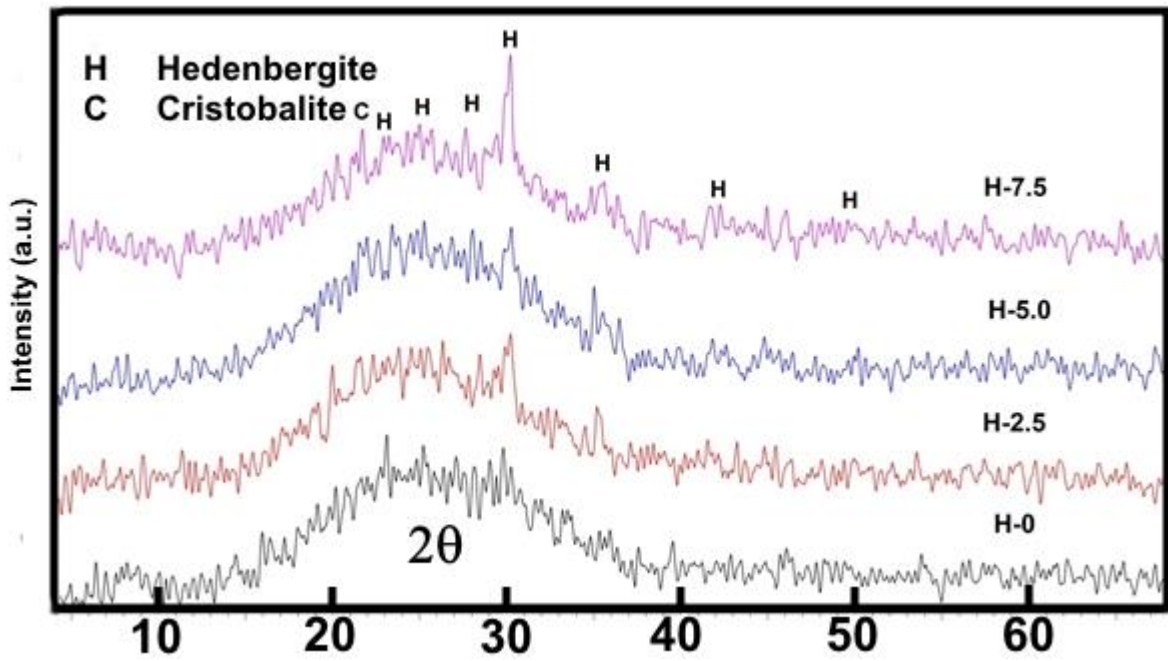


Fig.6

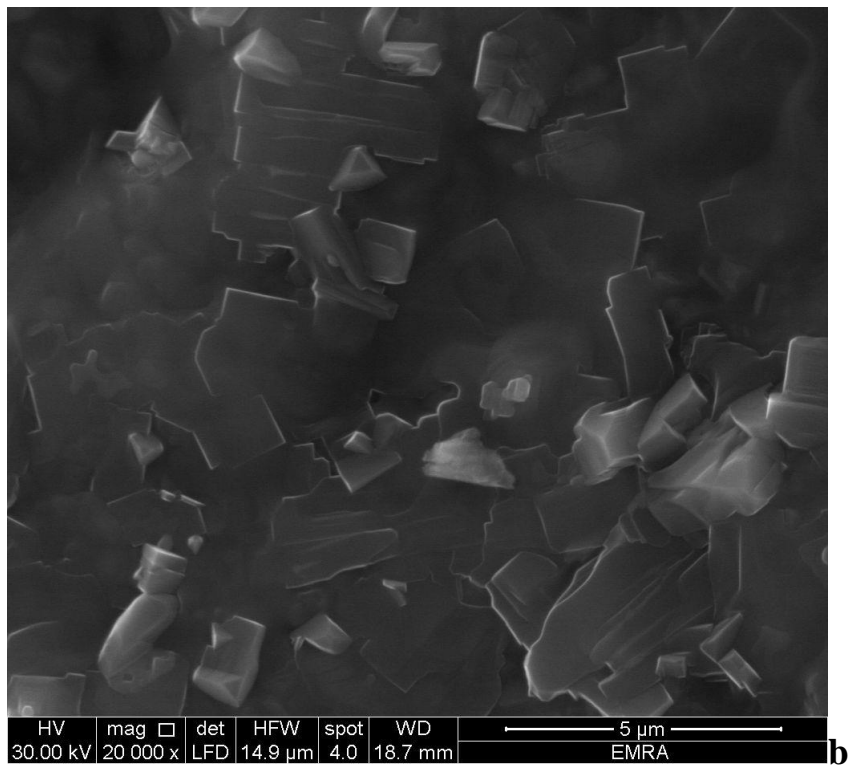
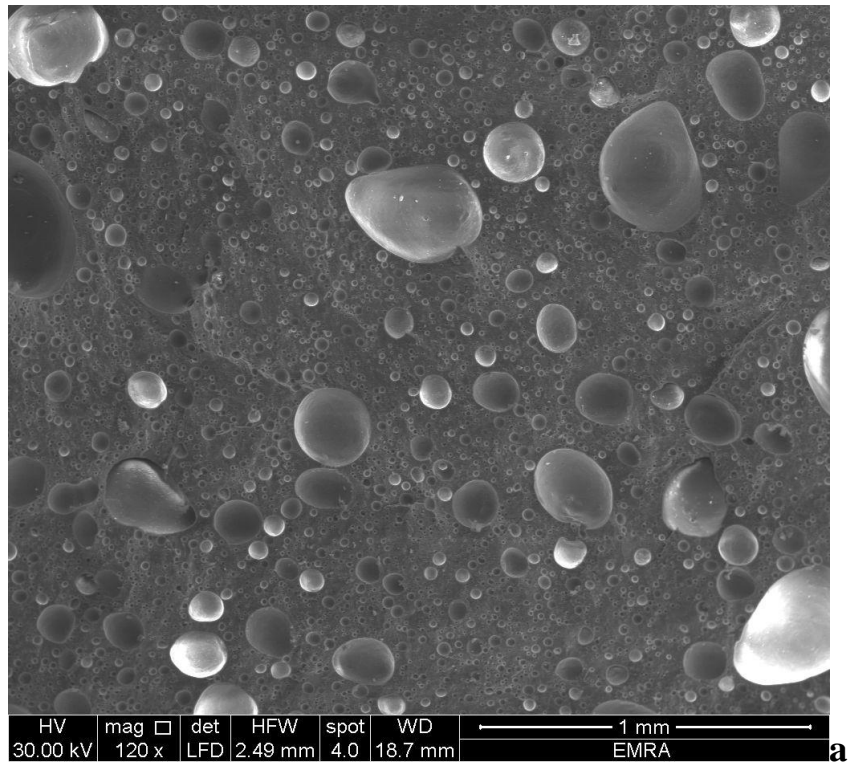


Fig. 7

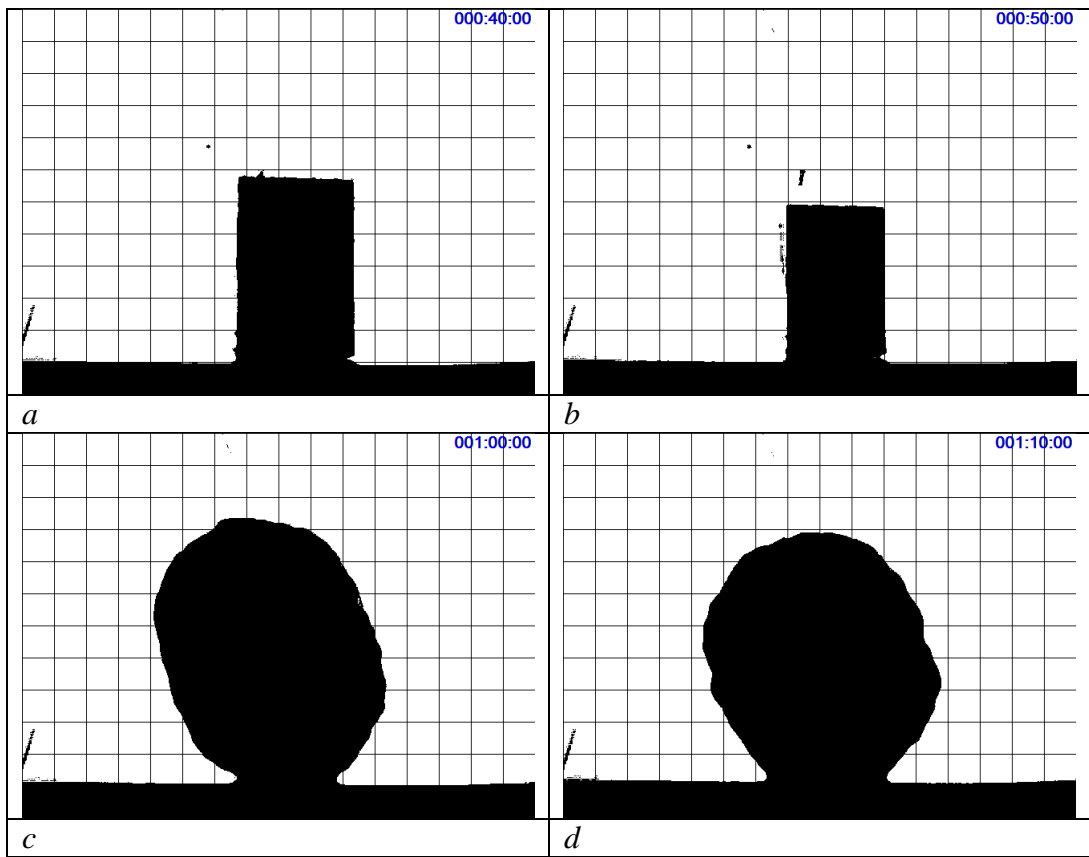
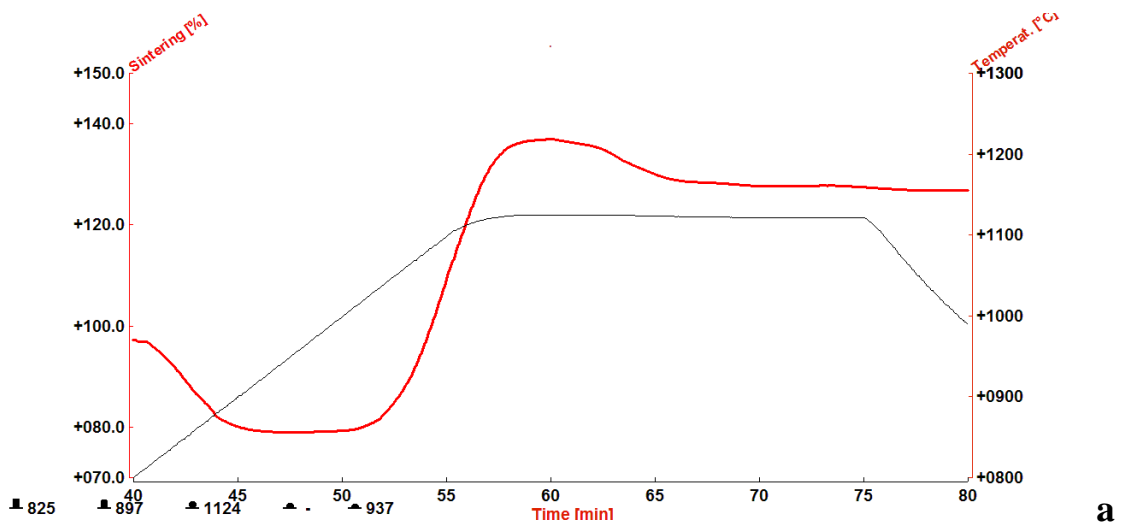


Fig. 8

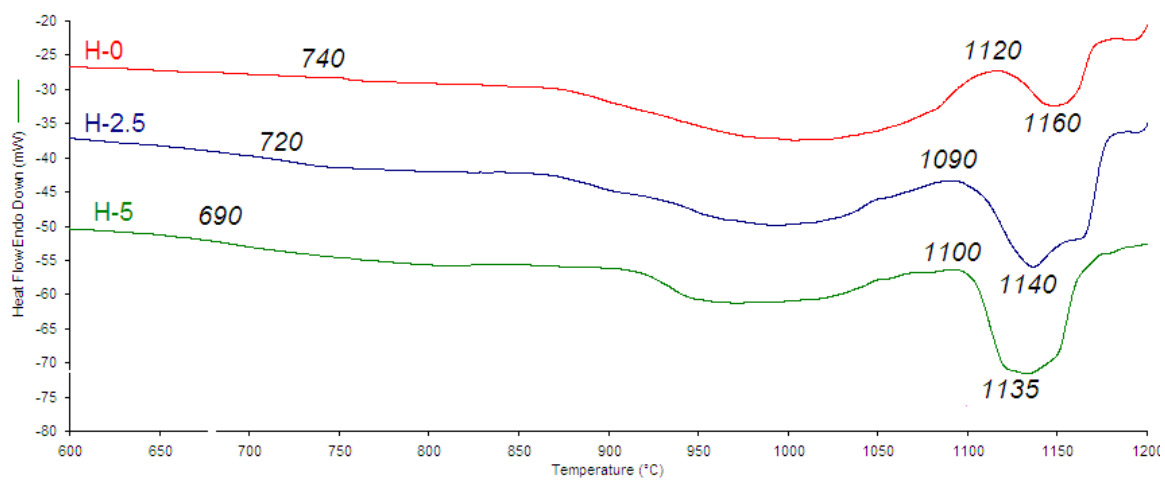


Fig. 9

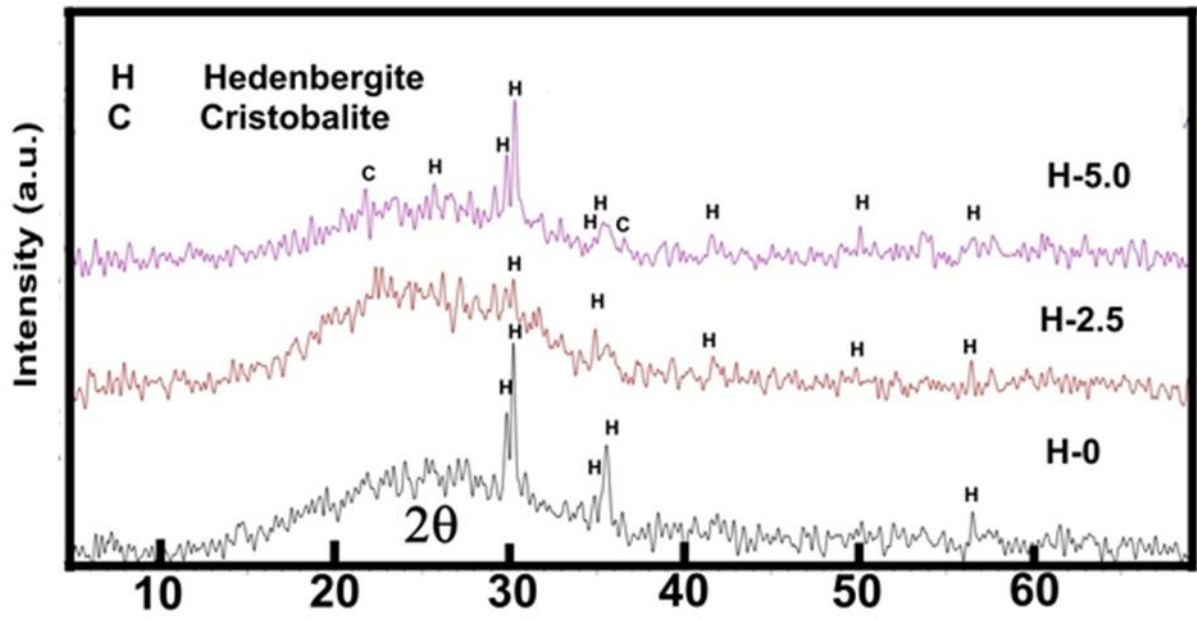
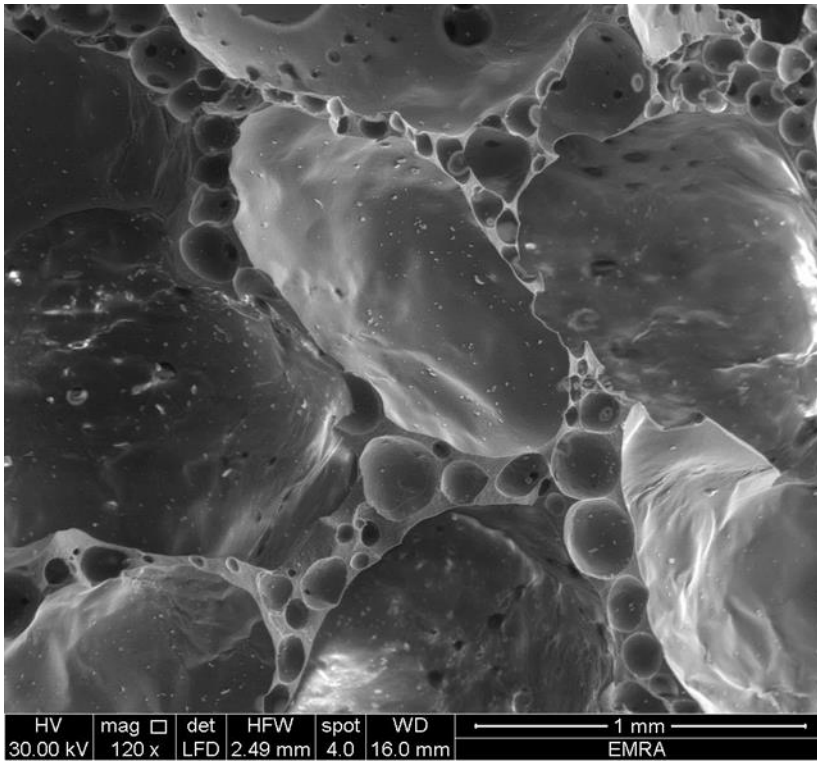
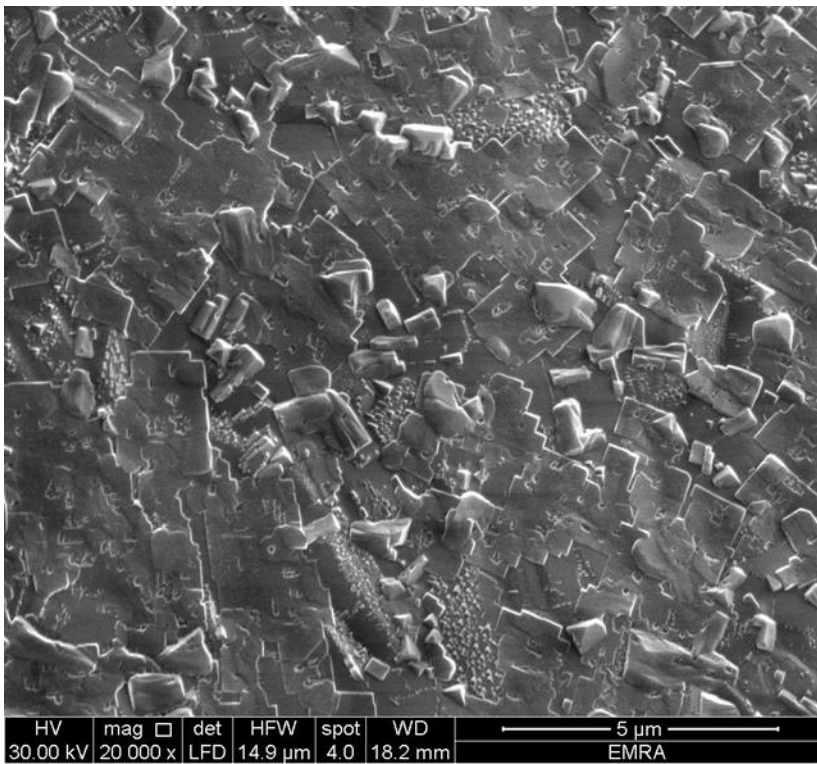


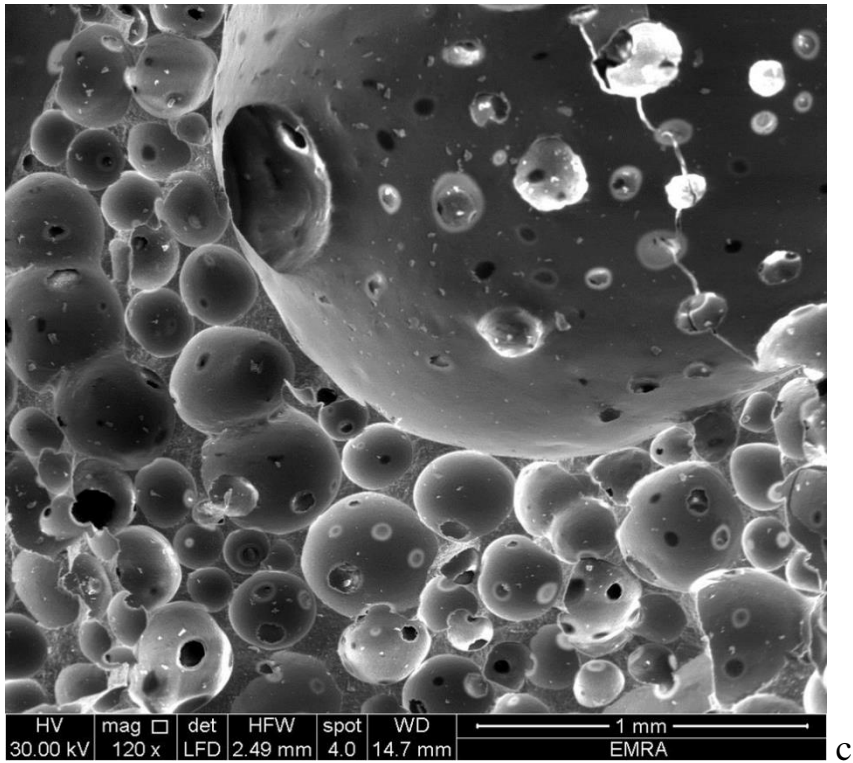
Fig. 10



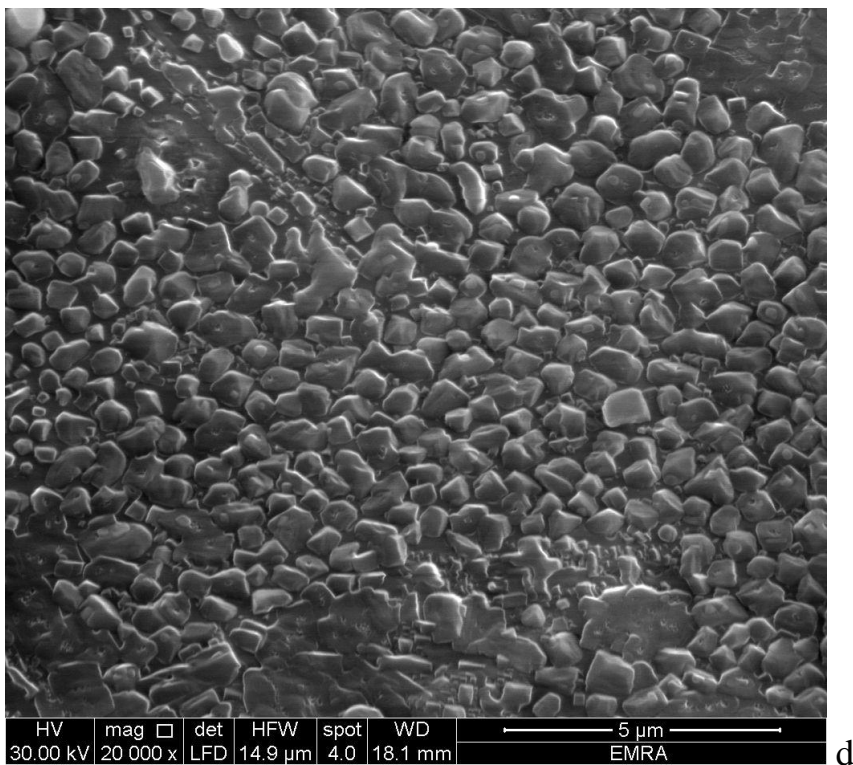
a



b



c



d

Fig. 11